Classification: Biological Sciences, Developmental Biology

Real-time imaging of the somite segmentation clock: revelation of unstable oscillators in the individual presomitic mesoderm cells

Yoshito Masamizu[1], Toshiyuki Ohtsuka[1], Yoshiki Takashima[1], Hiroki Nagahara[2], Yoshiko Takenaka[2], Kenichi Yoshikawa[2], Hitoshi Okamura[3], and Ryoichiro Kageyama[1,4]

[1]Institute for Virus Research, Kyoto University, Kyoto 606-8507, Japan; [2]Department of Physics, Kyoto University Graduate School of Science, Kyoto 606-8502, Japan; [3]Department of Brain Sciences, Kobe University Graduate School of Medicine, Kobe 650-0017, Japan

[4]Corresponding author: Ryoichiro Kageyama
Institute for Virus Research, Kyoto University
Shogoin-Kawahara, Sakyo-ku
Kyoto 606-8507, Japan
Tel: 81-75-751-4011 Fax: 81-75-751-4807
E-mail: rkageyam@virus.kyoto-u.ac.jp

The number of text pages: 16 The number of figures: 5

The number of words in the abstract: 150

The total number of text characters: 26,388

Abbreviations: PSM, presomitic mesoderm

Abstract

Notch signaling components such as the bHLH gene *Hes1* are cyclically expressed by negative feedback in the presomitic mesoderm (PSM) and constitute the somite segmentation clock. Because Hes1 oscillation occurs in many cell types, this clock may regulate the timing in many biological systems. While the Hes1 oscillator is stable in the PSM, it damps rapidly in other cells, suggesting that the oscillators in the former and the latter could be intrinsically different. Here, we have established the real-time bioluminescence imaging system of Hes1 expression and found that, although the Hes1 oscillation is robust and stable in the PSM, it is unstable in the individual dissociated PSM cells, as in fibroblasts. Thus, the Hes1 oscillators in the individual PSM cells and fibroblasts are intrinsically similar, and these results, together with mathematical simulation, suggest that the cell-cell communication is essential not only for synchronization but also for stabilization of cellular oscillators.

Introduction

Somites, precursors for the segmental structures such as the vertebral column, ribs and skeletal muscles, are generated in a head-to-tail order by periodic segmentation of the anterior end of the presomitic mesoderm (PSM). This periodic event is regulated by the somite segmentation clock, which is composed of Notch and Wnt signaling molecules (1-6). In the PSM, the Notch components such as the basic helix-loop-helix genes *Hes1* and *Hes7* are cyclically expressed, and each cycle leads to segmentation of a bilateral pair of somites (7-11). This oscillatory expression occurs in a synchronous manner but with the caudal-to-rostral phase delay, resulting in wave-like propagation of the expression domains from the caudal to rostral direction. It has been shown that this oscillatory expression depends upon a negative feedback loop (12-18).

Interestingly, Hes1 oscillation occurs in many cell types in addition to the PSM after serum treatment or activation of Notch signaling, suggesting that this clock may regulate the timing in many biological systems (12). While Hes1 oscillation is stable in the PSM, it is damped after three to six cycles in other cells, raising the possibility that the Hes1 oscillator of the PSM cells is intrinsically different from that of other cell types (8, 12). However, the damping could result not only from damped oscillation in each cell but also from desynchronization between cells, and it is not clear which is the case. It was shown that the PSM cells could become desynchronized when they are dissociated (19), but the nature of the segmentation clock in individual PSM cells remains to be determined.

In order to understand the dynamics of the somite segmentation clock, we attempted real-time imaging of Hes1 expression in the PSM and the dissociated individual PSM cells. Here, we found that the Hes1 oscillation is stable (both the period and amplitude are relatively constant) in the PSM but unstable (the period and amplitude are variable) in the individual dissociated PSM cells. The Hes1 oscillators in the individual dissociated

PSM cells are intrinsically similar to those in fibroblasts that are unstable in both the period and amplitude. These results indicate that the cell-cell communication is essential not only for synchronization but also for stabilization of cellular oscillators. This effect is also simulated by a mathematical model.

Results and Discussion

Since the half-life of Hes1 protein is about 20 min (12), that of the reporter should be 20 min or less. Otherwise, the reporter protein would be accumulated after several cycles of oscillation. In addition, since each peak comes about one hour after the trough, the reporter should become active immediately after induction. To overcome these problems, we used the ubiquitinated firefly luciferase as a reporter, which was previously shown to react to such rapid synthesis and degradation processes (20). This luciferase was fused at the amino-terminus with one (Ub1-Luc) or two copies (Ub2-Luc) of a mutant ubiquitin (G76V) that resists cleavage by ubiquitin hydrolases (20). Both reporter genes were driven by the 2.5-kb *Hes1* promoter (Fig. 1a), which contains sites for both Notch induction and negative feedback (Fig. 6).

We first generated clones of C3H10T1/2 fibroblasts stably transfected with each reporter and measured their bioluminescence. Treatment with cycloheximide, a translational inhibitor, showed that both Ub1-Luc and Ub2-Luc proteins were degraded with the half-lives of approximately 10 min and 6 min, respectively, but became stabilized in the presence of the proteasome inhibitor MG132 (Fig. 1b). Luciferase activities of the transfectants carrying either reporter showed, at least, three cycles of oscillations after serum treatment (Fig. 1c and data not shown), like the endogenous Hes1 expression (12). These results indicated that both Hes1-Ub1-Luc and Hes1-Ub2-Luc reporters well mimic

the dynamics of the endogenous Hes1 expression. Analysis of the time course showed that the peak of the luciferase activities came around 40 min after serum treatment while that of the endogenous *Hes1* mRNA came around one hour after serum treatment (Fig. 1d). We also compared the endogenous *Hes1* intron expression, which is detectable only when the gene is actively transcribed because the intron sequences are present only in nascent transcripts (15, 21). The peak of the *Hes1* intron expression came around 40 min after serum treatment (Fig. 1d). Thus, the reporter expression was as rapid as the endogenous *Hes1* intron expression, probably because the reporters do not have any introns and are much shorter in length than the endogenous *Hes1* gene. This result also pointed to the significant time delays in production of both *Hes1* mRNA and Hes1 protein, which were proposed as essential mechanisms for stable oscillatory gene expression (22, 23).

Using the stable transfectants described above, we attempted single-cell imaging of Hes1 expression after serum treatment. Bioluminescence was measured with a highly sensitive cooled CCD camera, as previously described (24). A total of 48 cells were monitored, and approximately 44% of the cells (n = 21) were found to exhibit short responses, one or two cycles, and then become almost silenced (Fig. 2a,b), while the others (56%, n = 27) showed longer responses: they were cycling over 12-hour period (Fig. 2c,d and Movie 1). The period and amplitude of each cycle were variable, and the average period was 122 ± 2 min. Strikingly, still many cells showed oscillation 36 hours after serum treatment. Most of them were cycling in an unstable manner while a few of them in a relatively stable manner (Fig. 2e,f and data not shown). Thus, the damped oscillation observed in cultured cells is not due to damped oscillation in all individual cells but due to desynchronization between the cycling cells. We also found that in the absence of serum treatment, many cells were cycling unsynchronously (data not shown), indicating that the oscillation goes unnoticed in untreated cultured cells because of desynchronization.

We next generated transgenic mice carrying the Hes1-Ub1-Luc reporter. The caudal part of the E10.5 transgenic embryo was cultured, and bioluminescence in the PSM was monitored. Hes1 is expressed at a high level in the somite 0 (S0) and at a lower level in the other PSM region (8). Real-time imaging showed that Hes1 oscillation was propagated from the caudal end to S0 in the PSM (Figs. 3a and 7 and Movie 2) and that each cycle generated a pair of somites (Fig. 3c). The caudal region was always earlier in phase than the rostral region (Fig. 3b, compare regions 1 and 2). During the 15-hour period, the Hes1 oscillator in the PSM was stable in both the period and amplitude (Fig. 3b) with the average period of about 160 min in our condition. This period was longer than that of Hes1 oscillation and somite segmentation seen in utero (about 120 min). We were reproducibly able to monitor the stable Hes1 oscillation and the somite segmentation for 15 hours, but after that the growth of the PSM was severely reduced and the boundaries of the somites became ambiguous, although Hes1 oscillation was still robust and stable even after one day.

It was previously shown that expression of the chick homolog *c-hairy1* oscillates even in dissected PSM fragments, suggesting that this oscillator functions in a cell-autonomous manner (7, 19). To confirm this result, we dissected the PSM of the Hes1-Ub1-Luc embryo into three fragments and monitored the bioluminescence of each fragment (Fig. 4a). Hes1 oscillation was stable in each fragment for about 9 hours (Fig. 4b,c), thus confirming the chick results. The caudal-to-rostral phase delay was lost at the first cycle after dissection but soon recovered from the second cycle onward within the same fragment (Fig. 4b, region 1 should be ahead of region 2). In contrast, the relative phase difference between the different fragments was not recovered after dissection (Fig. 4c, region 1 should be ahead of region 3 but became almost the same when separated). Thus, although the dissected PSM fragments maintain a stable Hes1 oscillator, they easily lose their relative phase difference when separated, suggesting that the direct or indirect cell-cell

communication is important to keep the precise phase difference.

It was recently shown that the dissociated PSM cells also become out of synchrony (19). However, it is not clear whether each PSM cell has a stable oscillator but is reset at various phases when dissociated or it has an unstable oscillator like fibroblasts. We thus next examined the Hes1 oscillation in dissociated PSM cells. Although Hes1 expression oscillated in each dissociated PSM cell (Fig. 4d,e and Movie 3), the period and amplitude were variable. The average period was 155 ± 6 min. Thus, the Hes1 oscillator in most if not all individual PSM cells is unstable in the period and amplitude, and this feature is very similar to that of the Hes1 oscillator in fibroblasts. These results suggest that the cell-cell communication may be important not only for synchronization but also for stabilization of cellular oscillators.

To see whether coupling of unstable cellular oscillators would be expected to form stable and synchronized oscillators, we simulated the Hes1 oscillation by adapting the model of stochastic coherence with coupling (for details, see Materials and Methods) (25-28). We assumed 128 unstable oscillators, which displayed random oscillatory expression (Figs. 5a and 8). In contrast, coupling by one-dimensional neighboring interaction made all these oscillators stabilized and synchronized (Fig. 5b). These results support the notion that the cell-cell communication could not only synchronize but also stabilize the unstable cellular oscillators

Our results indicate that the Hes1 oscillator of individual PSM cells is unstable and therefore intrinsically similar to that of fibroblasts. This result agrees well with the previous proposal that uncoupling of PSM cells could lead to random fluctuations of the oscillator expression in chick and zebrafish (19, 29). Thus, the coupling between cells is very important for an accurate biological clock and may be mediated by Notch signaling in the PSM, where cyclic Hes expression seems to be coupled by cyclic Notch activation (14,

29, 30). Because Notch signaling molecules are expressed in many developing tissues, such tissues might also have a stable and synchronized Hes1 oscillator, which could control the accurate timing in development. Our real-time imaging system would offer a powerful tool to look for such oscillating tissues.

Materials and Methods

Plasmids. The reporter constructs Hes1-Ub1-Luc and Hes1-Ub2-Luc were generated as follows. The coding region of one or two copies of ubiquitin G67V was fused to firefly luciferase cDNA in frame at the 5' terminus (gift of Dr. David Piwnica-Worms, Washington University School of Medicine) (20). The *Hes1* promoter and 5'UTR region (-2567 to +223), the Ub1-Luc/Ub2-Luc reporter, the *Hes1* 3'UTR (+2090 to +2453) and the downstream region (+2454 to +2626) were ligated in this order into pBluescript. The PGK-*neo* was also cloned at the 5' end of the *Hes1* promoter in reverse orientation for stable transfection.

Cell culture. C3H10T1/2 fibroblasts were transfected with the linearized Hes1-Ub1-Luc or Hes1-Ub2-Luc plasmid, using the FuGENE6 kit (Roche), according to the manufacturer's instructions. Neomycin-resistant clones were isolated by standard procedure and maintained in DMEM (GIBCO 11995-065), supplemented with 100U/ml penicillin, 100µg/ml streptomycin and 10% FBS at 37°C in 5% CO_2.

Promoter analysis. Hes1-Ub1-Luc or Hes1-Ub2-Luc (1µg) was transfected into NIH3T3 cells, which were plated in 6-multiwell plates at the density of 5 x 10^4 cells/ml, with or without 0.4µg of the expression vectors for Hes1 or the constitutively active form of Notch.

After 48 hours, the cells were harvested and luciferase activities were measured.

Real-time PCR. Real-time PCR was performed on the ABI PRISM 7300 Sequence Detection System using SYBR Green PCR Master Mix (Applied Biosystems) and 100nM each of primers. Primer sequences were designed as follows: for *Hes1* mRNA, the forward primer 5'-GGACAAACCAAAGACGGCCTCTGAGCACAG-3'; the reverse primer 5'-TGCCGGGAGCTATCTTTCTTAAGTGCATCC-3'; for *Hes1* intron expression, the forward primer 5'-AGTTGTTACTGCTCCGGAAATGGAGGGAGA-3'; the reverse primer 5'-CCTGCGGCAGGGGTTGGACCGGTGCTAAAC-3'; for glyceraldehyde-3-phosphate dehydrogenase (*GAPDH*), the forward primer 5'-ATCTTCTTGTGCAGTGCCAGCCTCGTCCCG-3'; the reverse primer 5'-AGTTGAGGTCAATGAAGGGGTCGTTGATGG-3'. Cycle conditions were 50°C for 2 min, 95°C for 10 min, and 60 cycles of 95°C for 15 sec and 60°C for 1 min. The specificity of the amplicon was assessed based on the dissociation curve profile. Quantification was determined by the threshold cycle. *GAPDH* was used as an internal control to normalize the expression.

Transgenic mice. The 5.1kb ClaI-NotI DNA fragment, which contains the *Hes1* promoter (-2567 to -1), *Hes1* 5'UTR (+1 to +223), *Ub1-Luc*, *Hes1* 3'UTR (+2090 to +2453) and the downstream region (+2454 to +2626), was isolated and injected into the male pronucleus. Genotyping of the Hes1-Ub1-Luc transgenic mice was performed by southern blot analysis. The region from –374 to +46 of the *Hes1* gene was used as a probe. A wild-type band with the size of 6.4kb and a band of the transgene with the size of 2.8kb were detected by this probe after digestion with HindIII. All animals used for this study were maintained and handled according to the protocols approved by Kyoto University.

Bioluminescence imaging of C3H10T1/2 cells. Cells were plated into 35mm glass based dishes (ø12mm glass, IWAKI 3911-035) with 1ml of DMEM with 0.2% FBS and 1mM Luciferin (Nacalai) for one day at 37°C in 5% CO_2, and the serum was increased to 5-20%. Then, the dish was placed on the stage of inverted microscope (Olympus IX81) and maintained at 37°C in 5% CO_2. Luminescence from the sample was collected by Olympus 20x UPlanApo objective (NA 0.8) and transmitted directly to a cooled CCD camera (Princeton Instruments VersArray 1KB). The signal-to-noise ratio was increased by 8 x 8 binning and 10 min exposure.

Bioluminescence imaging of the PSM. For imaging of the PSM, the caudal part of the E10.5 transgenic embryo was transferred into 35mm glass based dishes with 200µl of 100% rat serum with 1mM Luciferin and maintained at 37°C in 5% CO_2 and 85% O_2. Luminescence from the sample was collected by an Olympus 20x UPlanApo objective and transmitted directly to a cooled CCD camera. The signal-to-noise ratio was increased by 4 x 4 binning and 20 min exposure. Under this condition, we were reproducibly able to monitor the stable Hes1 oscillation and the somite segmentation for 15 hours. For imaging of the dissected PSM, we were able to monitor the Hes1 oscillation only for 9 hours because the fragments became degenerated after that.

Bioluminescence imaging of the dissociated PSM cells. The PSM without S0 region was dissected from the E9.5-E10.5 transgenic embryos and dissociated by brief exposure to trypsin (5 min at 37°C) and mechanical pipetting, as previously described (19). The dissociated cells were then re-suspended in 200µl of 100% rat serum with 1mM Luciferin to inhibit the trypsin. This cell suspension was plated in 35mm poly-L-lysine-coated glass based dishes and maintained at 37°C in 5% CO_2 and 85% O_2. Luminescence from the

sample was collected by an Olympus 40x UPLFLN objective (NA 1.3) and transmitted directly to a cooled CCD camera. The signal-to-noise ratio was increased by 8 x 8 binning and 10 min exposure.

Image analysis. Images were analyzed with Image-Pro Plus (Media Cybernetics, Inc.). Cosmic ray-induced background noise in the image data was removed. Luminescence intensity was measured within a region of interest defined manually for each cell. The position of the region was adjusted if necessary to accommodate movements of cells during the experiment. Data were logged to Microsoft Excel files for plotting and further analysis. Data were corrected for bias by subtracting average luminescence intensity in no-cell region. When measuring the period of oscillations, changes with more than 15% of the biggest peak-trough difference were considered, while smaller and abrupt changes (mostly less than 10% of the biggest) may be due to stochastic fluctuation and therefore excluded.

Mathematical modeling. In order to reproduce the experimental trend by numerical simulation, we adapted the model of stochastic coherence with coupling (25-28). Let r_i be a parameter to represent the state of DNA in the i th cell, where $r_i = 1$ and $r_i = 0$ represent the active and inactive states, corresponding to the swelled and compact states, respectively, in the packing of the DNA domain for the related genes (27, 28). Let p_i be the number of Hes1 proteins for the i th cell. The rates of the changes of r_i and p_i are simply expressed as follows:

$$\frac{dr_i}{dt} = \frac{1}{\varepsilon_1} f(r_i, p_i) + \sqrt{2D_1}\xi_{i,1} + k_3(r_{i+1} + r_{i-1} - 2r_i) \qquad \text{(a)}$$

$$\frac{dp_i}{dt} = \frac{1}{\varepsilon_2} g(r_i, p_i) + \sqrt{2D_2}\xi_{i,2} \qquad \text{(b)}$$

$$f(r_i, p_i) = r_i(r_i - \frac{1}{2})(1 - r_i) - k_1(p_i - k_2) \qquad \text{(c)}$$

$$g(r_i, p_i) = (r_i - k_4) - k_5 p_i \qquad \text{(d)}$$

where the functions $f(r_i, p_i)$ and $g(r_i, p_i)$ represent the local reactions with time constants ε_1 and ε_2. As the stochastic stimulus, we introduced additive white noises $\xi_{i,1}$ and $\xi_{i,2}$, which are uncorrelated each other ($\left\langle \xi_{i,m}(t)\xi_{j,n}(t') \right\rangle = \delta_{ij}\delta_{mn}\delta(t-t')$, $m, n = 1,2$). The third term in the right-hand side of the equation (a) represents the neighbor interaction with the strength of k_3. Throughout the simulations, we set $k_1 = 0.20$, $k_2 = 0.40$, $k_4 = 0.050$, $k_5 = 0.75$, $\varepsilon_1 = \frac{1}{1024}$, $\varepsilon_2 = \frac{1}{2}$ and $D_1 = D_2 = 2.0 \times 10^{-4}$. An uncoupled oscillator ($k_3 = 0$) indicates an intermittent behavior (Fig. 8). Fig. 5 shows the time evolutions of the arrays of 128 cells without and with the neighbor interaction. When k_3 is set to be zero, each individual cell independently behaves as fluctuating oscillator (Figs. 5a and 8). When k_3 is set to be 12, all the cells oscillate in a synchronized manner (Fig. 5b).

Acknowledgements

We thank D. Ish-Horowicz and O. Pourquié for critical reading of the manuscript, D. Piwnica-Worms for the ubiquitin-luciferase reporter and S. Yamada for production of transgenic mice. This work was supported by the Genome Network Project and the Scientific Research on Priority Areas from the Ministry of Education, Culture, Sports, Science and Technology of Japan, Yamanouchi Foundation and Uehara Memorial Foundation.

References

1. Pourquié, O. (2003) *Science* **301,** 328-330.
2. Bessho, Y. & Kageyama, R. (2003) *Curr. Opin. Genet Dev.* **13,** 1678-1690.
3. Weinmaster, G & Kintner, C. (2003) *Annu. Rev. Cell Dev. Biol.* **19,** 367-395.
4. Aulehla, A. & Herrmann, B.G. (2004) *Genes Dev.* **18,** 2060-2067.
5. Giudicelli, F. & Lewis, J. (2004) *Curr. Opin. Genet. Dev.* **14,** 407-414.
6. Rida, P.C.G., Minh, N.L. & Jiang, Y.-J. (2004) *Dev. Biol.* **265,** 2-22.
7. Palmeirim, I., Henrique, D., Ish-Horowicz, D. & Pourquie, O. (1997) *Cell* **91,** 639-648.
8. Jouve, C., Palmeirim, I., Henrique, D., Beckers, J., Gossler, A., Ish-Horowicz, D. & Pourquie, O. (2000) *Development* **127,** 1421-1429.
9. Holley S.A., Geisler, R. & Nüsslein-Volhard, C. (2000) *Genes Dev.* **14,** 1678-1690.
10. Sawada, A., Fritz, A., Jiang, Y.-J., Yamamoto, A., Yamasu, K., Kuroiwa, A., Saga, Y. & Takeda, H. (2000) *Development* **127,** 1691-1702.
11. Bessho, Y., Sakata, R., Komatsu, S., Shiota, K., Yamada, S. & Kageyama, R. (2001) *Genes Dev.* **15,** 2642-2647.
12. Hirata, H., Yoshiura, S., Ohtsuka, T., Bessho, Y., Harada, T., Yoshikawa, K. & Kageyama, R. (2002) *Science* **298,** 840-843.
13. Holley, S.A., Julich, D., Rauch, G.J., Geisler, R. & Nüsslein-Volhard, C. (2002) *Development* **129,** 1175-1183.
14. Dale, J.K., Maroto, M., Dequeant, M.L., Malapert, P., McGrew, M. & Pourquié, O. (2003) *Nature* **421,** 275-278.
15. Bessho, Y., Hirata, H., Masamizu Y. & Kageyama, R. Periodic repression by the bHLH factor Hes7 is an essential mechanism for the somite segmentation clock. *Genes Dev.* **17,** 1451-1456 (2003).
16. Hirata H., Bessho, Y., Kokubu, H., Masamizu, Y., Yamada, S., Lewis, J. & Kageyama,

R. (2004) *Nat. Genet.* **36,** 750-754.

17. Kawamura, A., Koshida, S., Hijikata, H., Sakaguchi, T., Kondoh, H. & Takada, S. (2005) *Genes Dev.* **19,** 1156-1161.
18. Morimoto, M., Takahashi, Y., Endo, M. & Saga, Y. (2005) *Nature* **435,** 354-359.
19. Maroto, M., Dale, J.K., Dequéant, M.-L., Petit, A.-C. & Pourquié, O. (2005) *Int. J. Dev. Biol.* **49,** 309-315.
20. Luker, G.D., Pica, C.M., Song, J., Luker, K.E. & Piwnica-Worms, D. (2003) *Nat. Med.* **9,** 969-973.
21. Morales, A.V., Yasuda, Y. & Ish-Horowicz, D. (2002) *Dev. Cell* **3,** 63-74.
22. Lewis, J. (2003) *Curr. Biol.* **13,** 1398-1408.
23. Monk, N.A.M. (2003) *Curr Biol.* **13,** 1409-1413.
24. Yamaguchi, S., Isejima, H., Matsuo, T., Okura, R., Yagita, K., Kobayashi, M. & Okamura, H. (2003) *Science* **302,** 1408-1412.
25. Hu, B. & Zhou, C. (2000) *Phys. Rev. E* **61**, R1001-R1004.
26. Han, S.K., Yim, T.G., Postnov, D.E. & Sosnovtseva, O.V. (1999) *Phys. Rev. Lett.* **83**, 1771-1774.
27. Yoshikawa, K. (2002) *J. Biol. Phys.* **28**, 701-712.
28. Yoshikawa, K. & Yoshikawa, Y. (2002) in *Pharmaceutical Perspectives of Nucleic Acid-Based Therapeutics*, R. I. Mahato, S. W. Kim, Eds. (Taylor & Francis, London), pp. 138-163.
29. Jiang, Y.-J., Aerne, B.L., Smithers, L., Haddon, C., Ish-Horowicz, D. & Lewis, J. (2000) *Nature* **408,** 475-479.
30. Huppert, S.S., Ilagan, M.X.G., De Strooper, B. & Kopan, R. (2005) *Dev. Cell* **8,** 677-688.

Figure legends

Fig. 1. Characterization of the Hes1 reporters. (**a**) Structures of the Hes1 reporters. (**b**) Bioluminescence of C3H10T1/2 fibroblasts stably transfected with Hes1-Ub1-Luc or Hes1-Ub2-Luc was measured in the presence of cycloheximide (20μM) (n = 3). Luminescence from Hes1-Ub1-Luc and Hes1-Ub2-Luc transfectants was decreased with the half-lives of approximately 10 min and 6 min, respectively, but became stabilized in the presence of the proteasome inhibitor MG132 (100μM). (**c**) The luciferase activity of Hes1-Ub2-Luc transfectants was measured after serum treatment. Three cycles of oscillation was observed. (**d**) The luciferase activity and *Hes1* mRNA and intron expression of Hes1-Ub1-Luc and Hes1-Ub2-Luc transfectants were measured after serum treatment.

Fig. 2. Bioluminescence imaging of C3H10T1/2 fibroblasts stably transfected with Hes1-Ub2-Luc. (**a**) Bioluminescence images of individual cells after serum treatment. Images were taken by 10 min exposure and binning of pixels 8 x 8 to increase the signal-to-noise ratios. (**b**) Quantification of bioluminescence of individual cells shown in (**a**). (**c**) Bioluminescence images of individual cells after serum treatment (see Movie 1). (**d**) Quantification of bioluminescence of individual cells shown in (**c**). (**e**) Bioluminescence images of an individual cell 36 hours after serum treatment. (**f**) Quantification of the bioluminescence of an individual cell shown in (**e**).

Fig. 3. Bioluminescence imaging of the PSM of a Hes1-Ub1-Luc embryo. (**a**) Bioluminescence images of the PSM were taken by 20 min exposure and binning of pixels 4 x 4 (see Movie 2). Asterisk in the top left panel indicates S0. Hes1 oscillation was propagated from the caudal end to S0. (**b**) Quantification of bioluminescence in the PSM. Oscillation was stable in both the period and amplitude. Region 1 is always earlier in phase

than region 2. (**c**) Bright field exposure. After 15-hour incubation, six new somites were segmented (arrowheads).

Fig. 4. Bioluminescence imaging of the dissected PSM fragments and dissociated PSM cells of Hes1-Ub1-Luc embryos. (**a**) The caudal part was dissected into three fragments. (**b**) Quantification of bioluminescence of regions 1 and 2. After the second cycle onward, region 1 was ahead of region 2, thus recovering the phase difference. (**c**) Quantification of bioluminescence of regions 1 and 3. The phase difference between regions 1 and 3 was not recovered. (**d**) Bioluminescence images of the individual dissociated PSM cells (see Movie 3). Images were taken by 10 min exposure and binning of pixels 8 x 8 to increase the signal-to-noise ratios. (**e**) Quantification of bioluminescence of individual PSM cells shown in (**d**).

Fig. 5. Mathematical simulations for the uncoupled and coupled oscillators. (**a**) Mathematical simulation for the uncoupled condition. The time course of 128 unstable oscillators is presented on the left. The trough and peak are shown in black and white, respectively. Three representative oscillators (#32, 64, 96) are shown on the right. (**b**) Mathematical simulation for the coupled condition. One-dimensional neighboring interaction makes all the oscillators stabilized and synchronized. Three representative oscillators (#32, 64, 96) are shown on the right.

Fig.1.

a

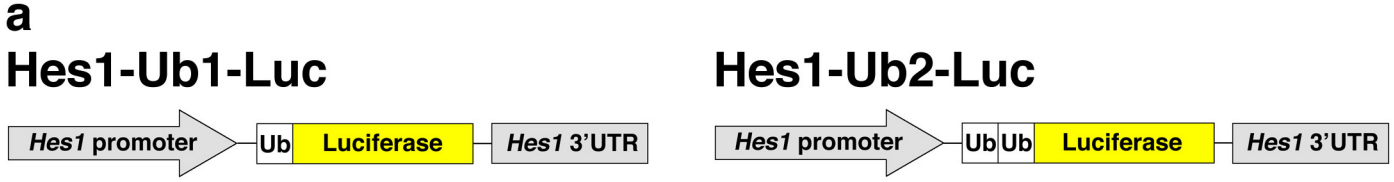
Hes1-Ub1-Luc
Hes1 promoter
Ub
Luciferase
Hes1 3'UTR
Hes1-Ub2-Luc
Hes1 promoter
Ub
Ub
Luciferase
Hes1 3'UTR

b

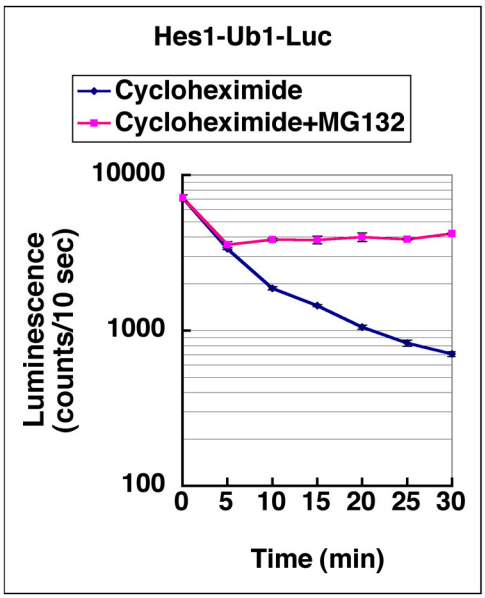
Hes1-Ub1-Luc
Cycloheximide
Cycloheximide+MG132
Luminescence (counts/10 sec)
10000
1000
100
0 5 10 15 20 25 30
Time (min)

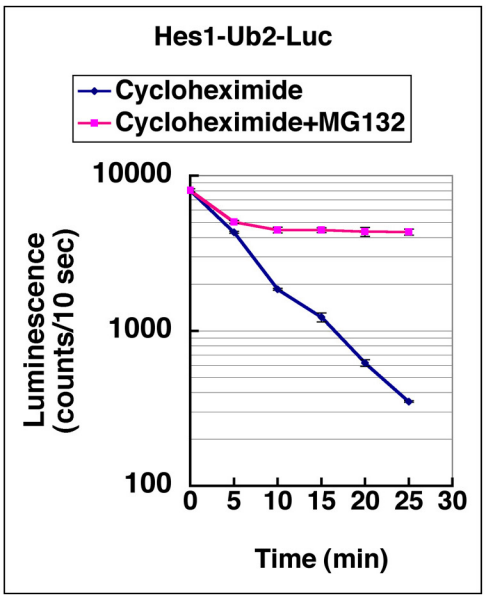
Hes1-Ub2-Luc
Cycloheximide
Cycloheximide+MG132
Luminescence (counts/10 sec)
10000
1000
100
0 5 10 15 20 25 30
Time (min)

c

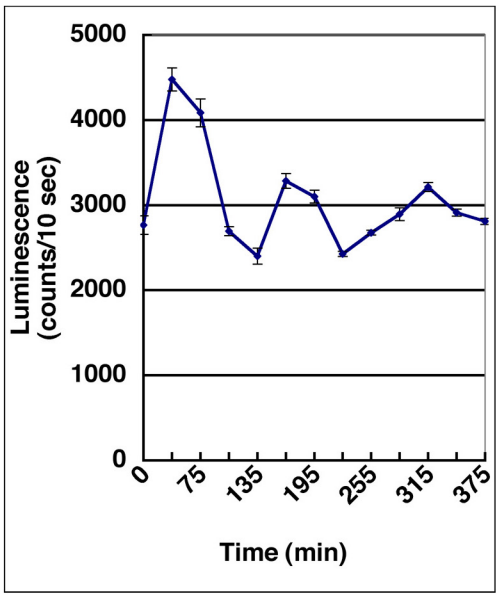
Luminescence (counts/10 sec)
5000
4000
3000
2000
1000
0
0 75 135 195 255 315 375
Time (min)

d

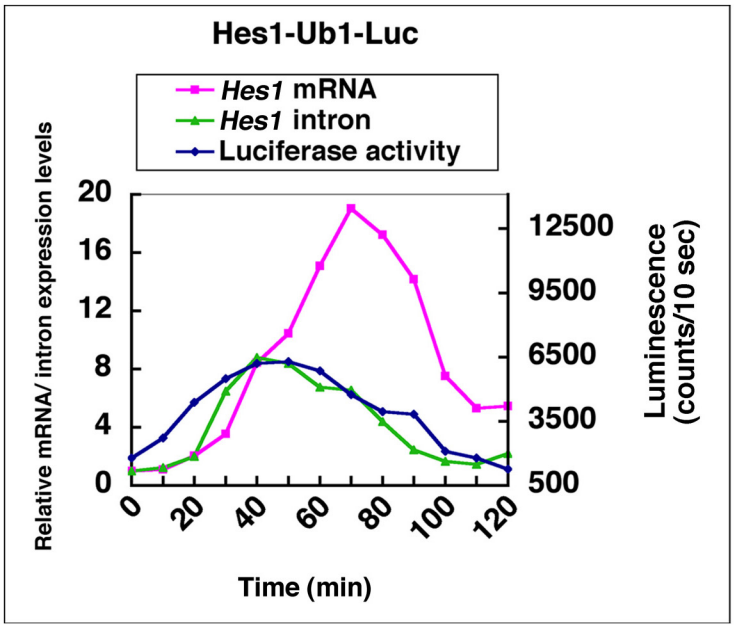
Hes1-Ub1-Luc
Hes1 mRNA
Hes1 intron
Luciferase activity
Relative mRNA/ intron expression levels
20
16
12
8
4
0
12500
9500
6500
3500
500
Luminescence (counts/10 sec)
0 20 40 60 80 100 120
Time (min)

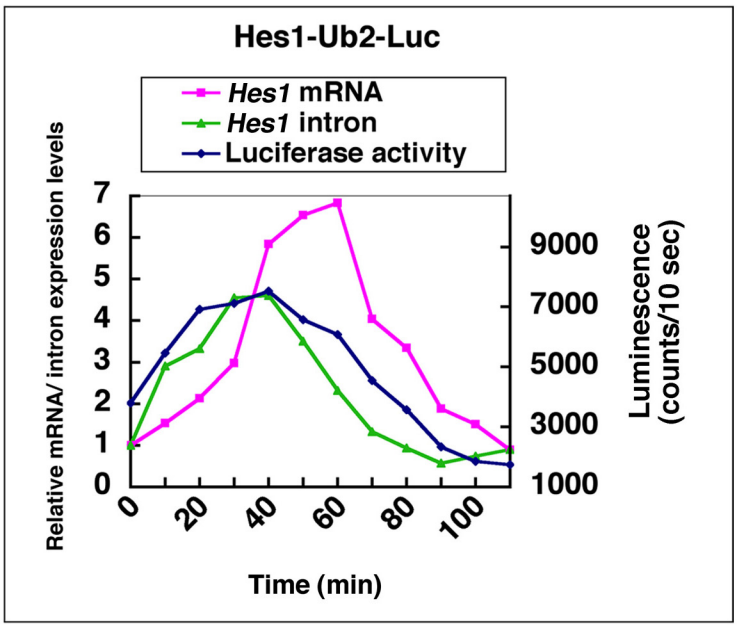
Hes1-Ub2-Luc
Hes1 mRNA
Hes1 intron
Luciferase activity
Relative mRNA/ intron expression levels
7
6
5
4
3
2
1
0
9000
7000
5000
3000
1000
Luminescence (counts/10 sec)
0 20 40 60 80 100
Time (min)

Fig.2.

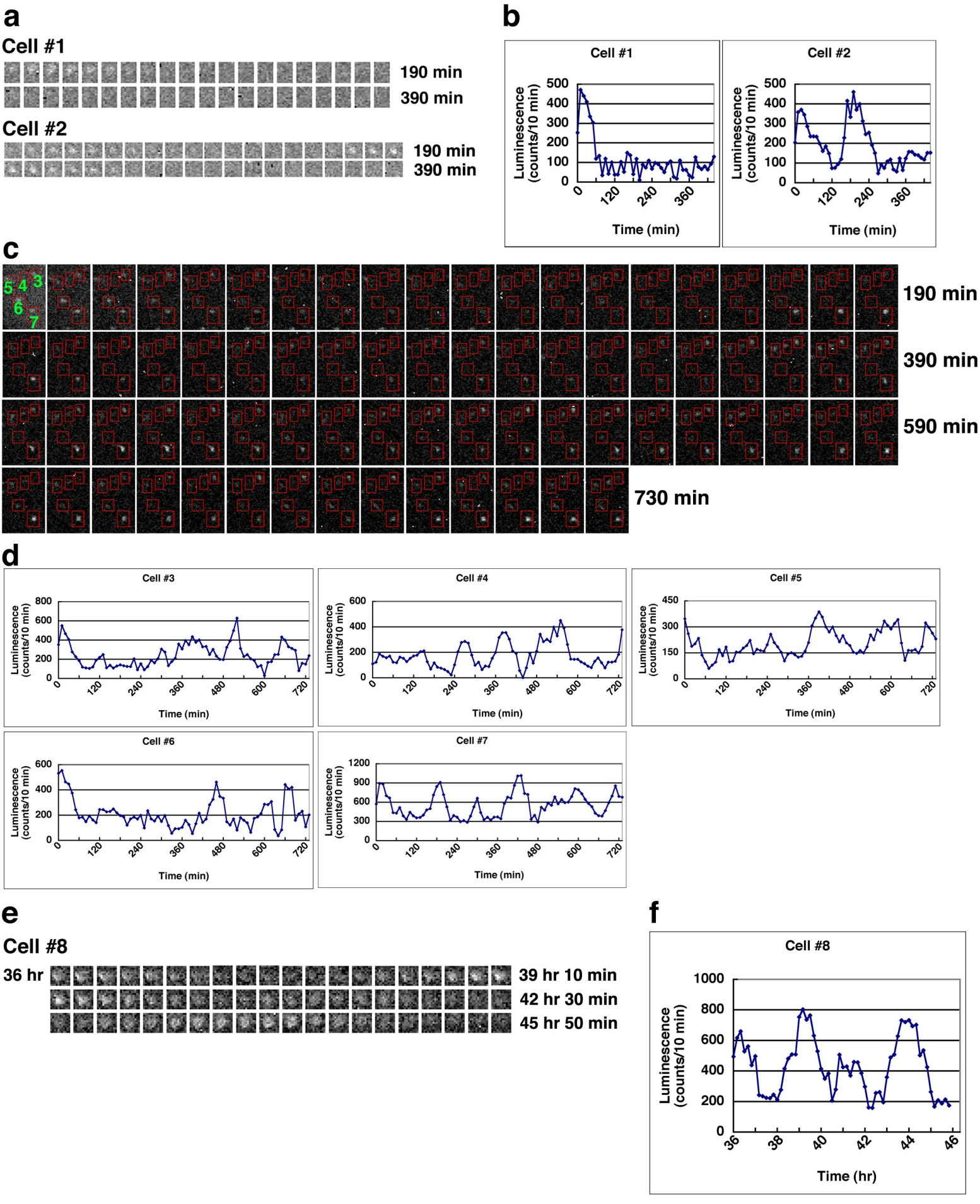
a
Cell #1
190 min
390 min
Cell #2
190 min
390 min
b
Cell #1
Cell #2
Luminescence (counts/10 min)
Time (min)
c
5 4 3
6
7
190 min
390 min
590 min
730 min
d
Cell #3
Cell #4
Cell #5
Cell #6
Cell #7
Luminescence (counts/10 min)
Time (min)
e
Cell #8
36 hr
39 hr 10 min
42 hr 30 min
45 hr 50 min
f
Cell #8
Luminescence (counts/10 min)
Time (hr)

Fig.3.

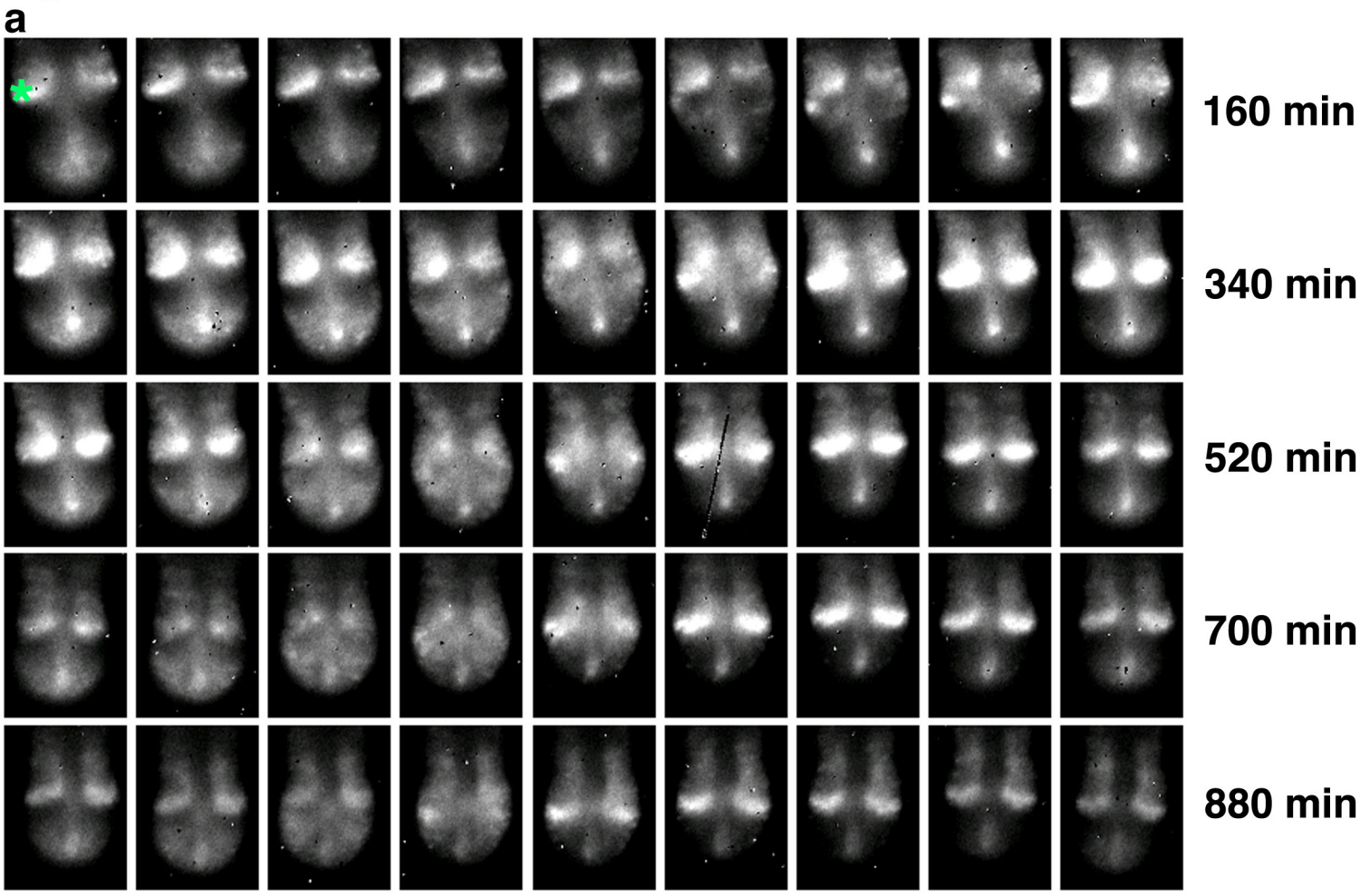
a
160 min
340 min
520 min
700 min
880 min
b
2
1
Region1
Region2
60000
40000
20000
0
Luminescence (counts/20 min)
0
120
240
360
480
600
720
840
Time (min)
c
t=0
t=15 hr

Fig.4.

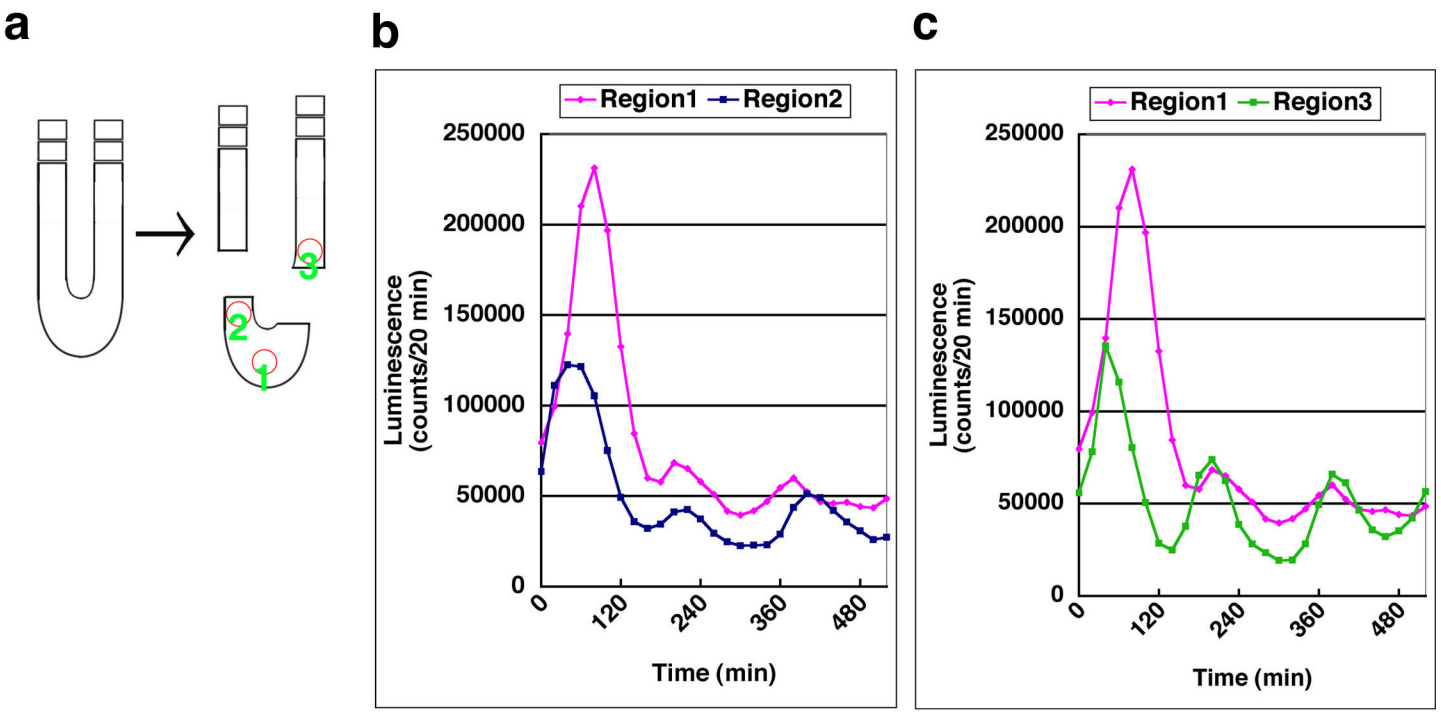
a
b
c
Region1
Region2
Region3
Luminescence (counts/20 min)
Time (min)
0
50000
100000
150000
200000
250000
0
120
240
360
480
1
2
3

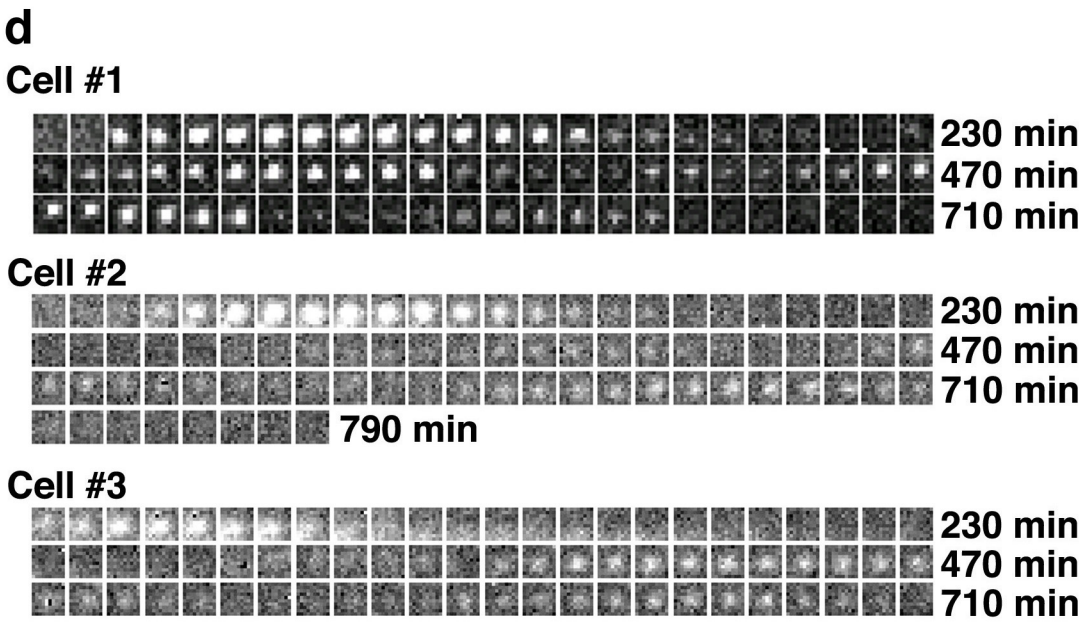
d
Cell #1
230 min
470 min
710 min
Cell #2
230 min
470 min
710 min
790 min
Cell #3
230 min
470 min
710 min

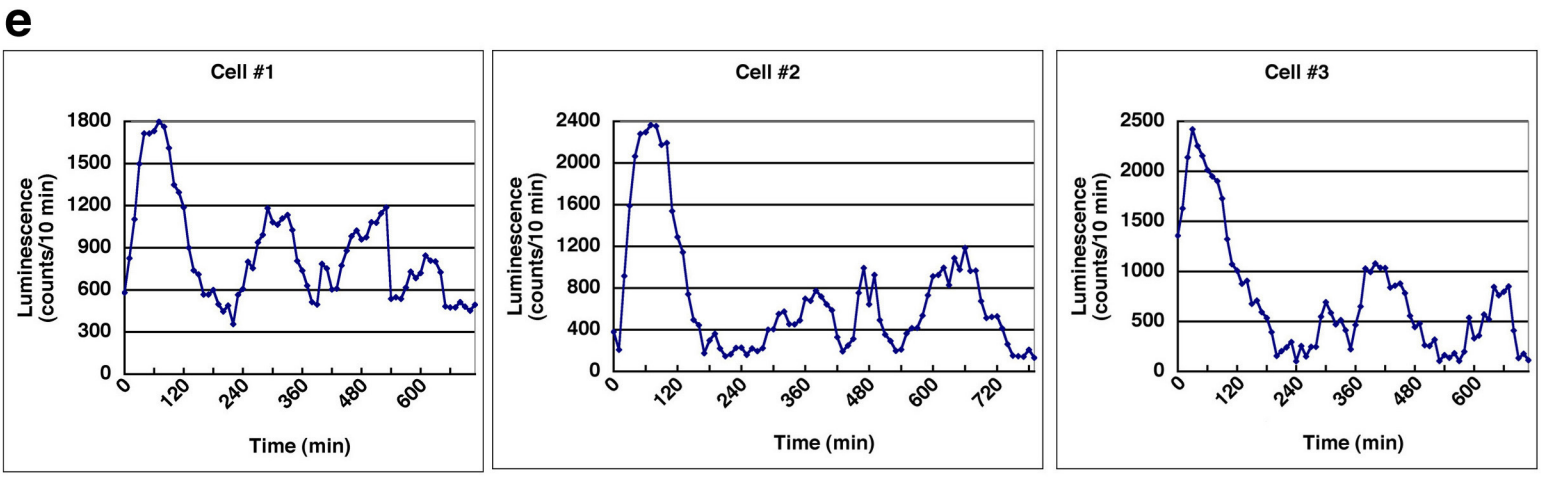
e
Cell #1
Cell #2
Cell #3
Luminescence (counts/10 min)
Time (min)
0
300
600
900
1200
1500
1800
400
800
1600
2000
2400
500
1000
2500
120
240
360
480
600
720

Fig.5.

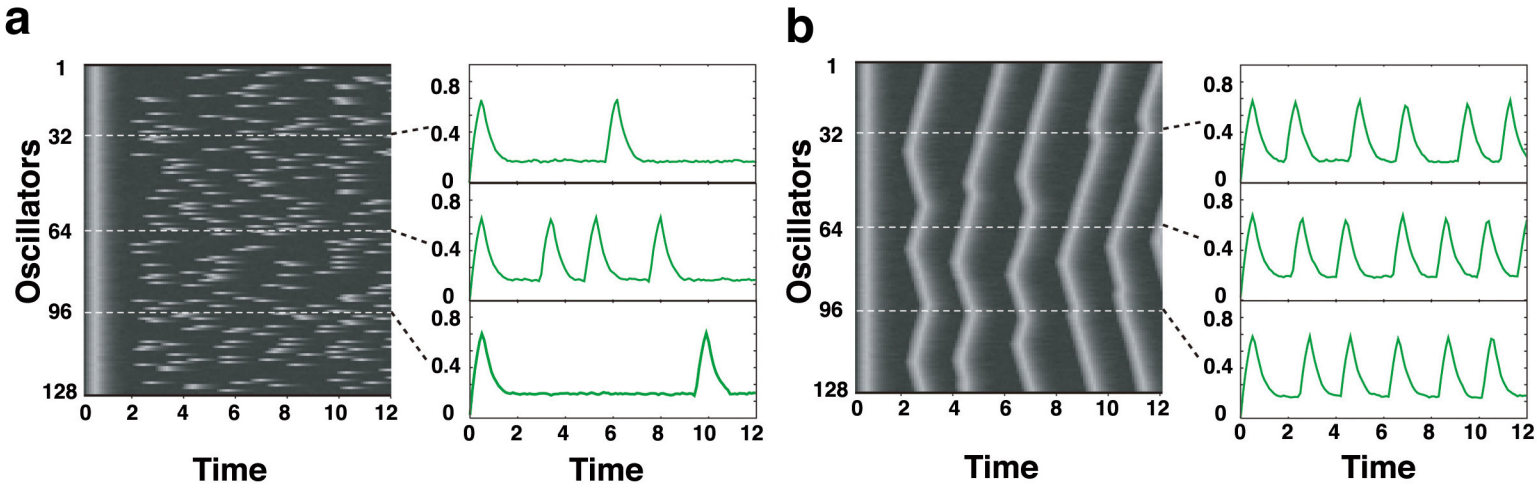

Supporting Information

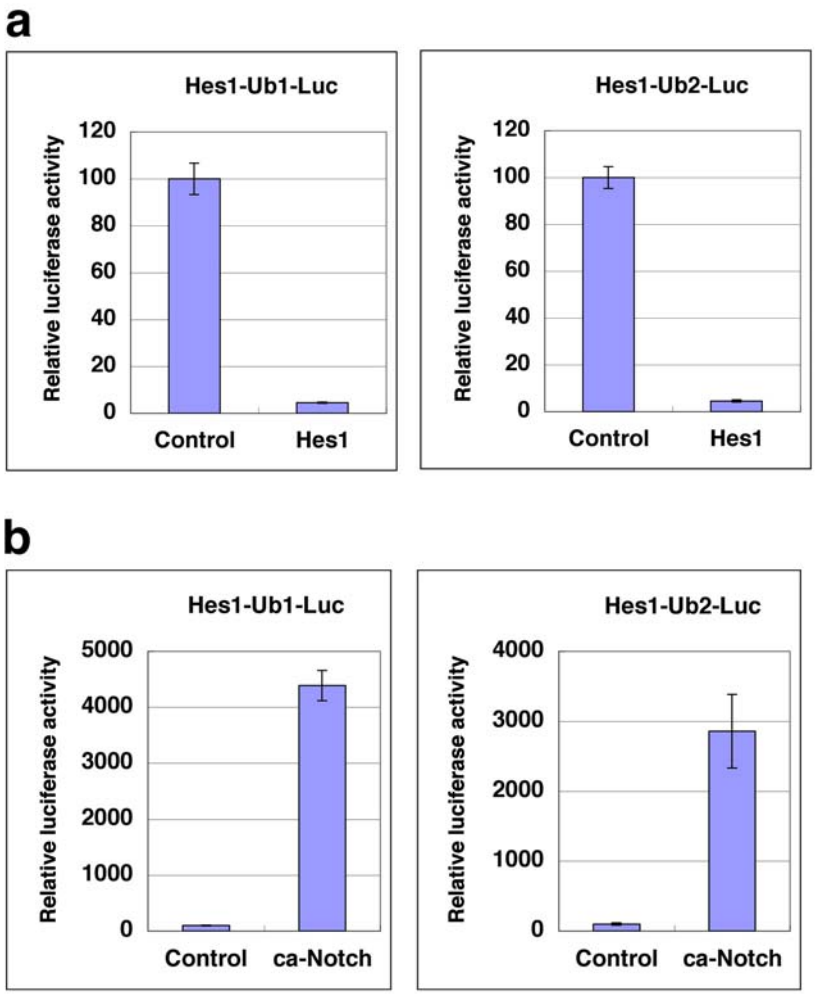

Figure 6. Regulation of *Hes1* promoter. (**a**) Co-transfection of Hes1-Ub1-Luc or Hes1-Ub2-Luc with the Hes1 expression vector showed significant reduction of the luciferase activity. (**b**) Co-transfection of Hes1-Ub1-Luc or Hes1-Ub2-Luc with the expression vector for a constitutive active form of Notch (ca-Notch) showed significant increase of the luciferase activity. Thus, the 2.5-kb *Hes1* promoter region contained sites for both Notch induction and negative feedback. The control luciferase activity was taken as 100, and the relative activities were measured (n = 3).

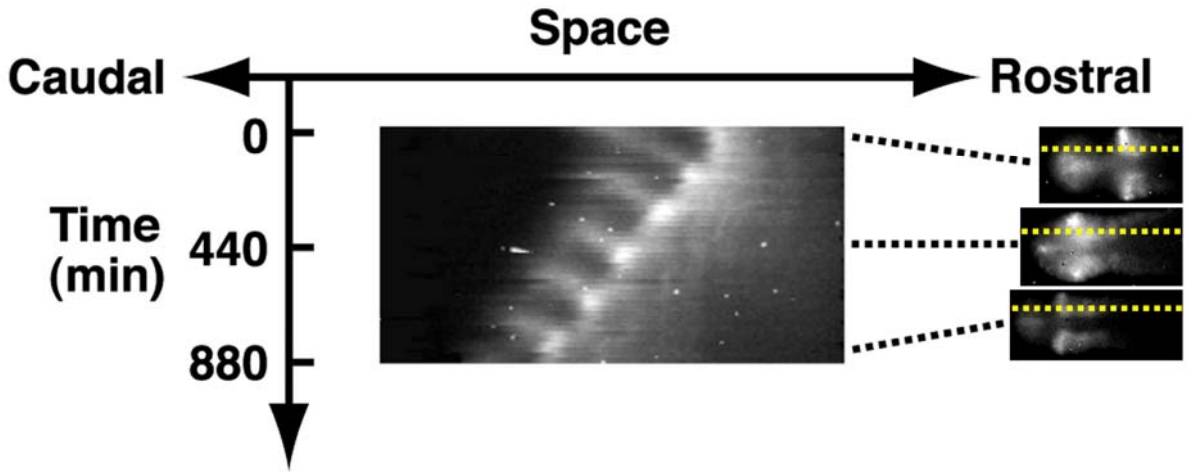

Figure 7. Spatio-temporal profiles of Hes1 oscillation in the PSM. The profiles were made from Fig. 3a. The bioluminescence intensity along the rostral-caudal axis (shown by yellow broken lines in three representative figures on the right) was plotted according to the time. Hes1 oscillation was propagated from the caudal end to S0. This propagation did not lose a finite velocity when it reached S0.

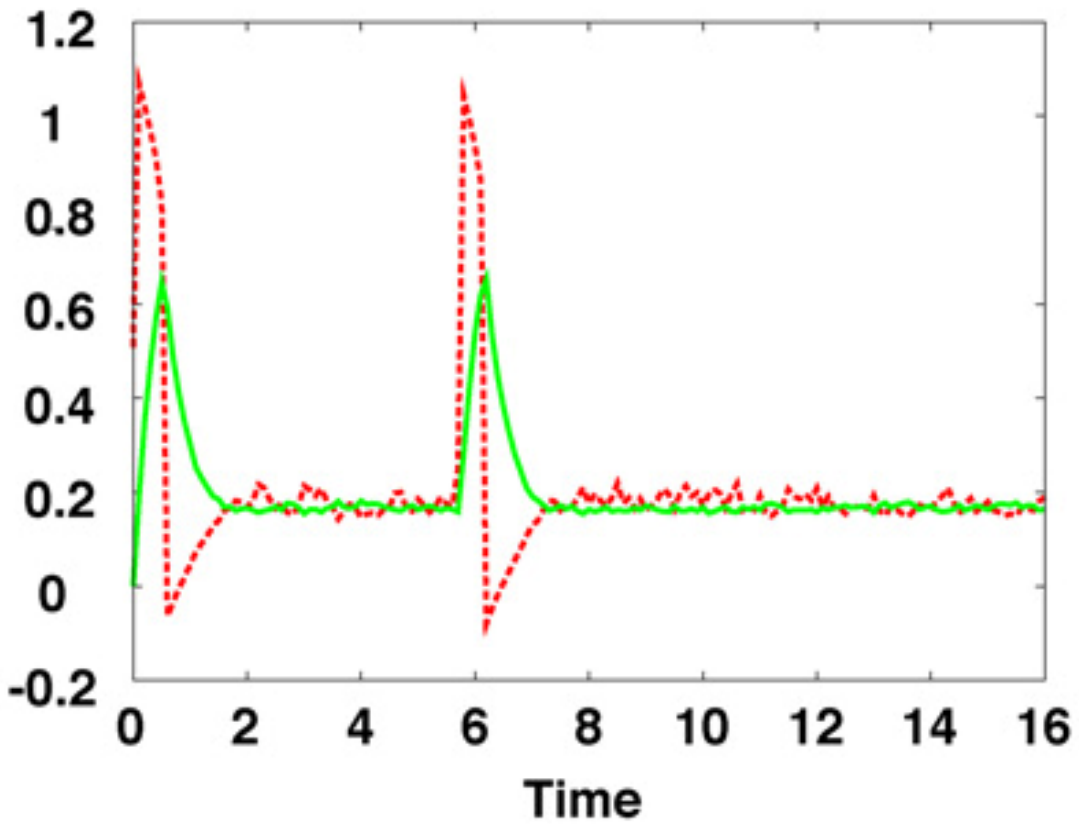

Figure 8. An example of the intermitted behavior of an uncoupled oscillator on the mathematical model Eqs. (a)-(d). The red broken and green solid lines correspond to the time changes of the order parameter of DNA (r_i) and the number of Hes1 proteins (p_i) in a single cell, respectively.

Movie legends

Movie 1. Real-time images of C3H10T1/2 cells stably transfected with Hes1-Ub2-Luc (#3-#7 in Fig. 2). Images were taken by 10 min exposure and binning of pixels 8 x 8 over a period of 12 hours following serum treatment. These cells were cycling but variable in the period and amplitude.

Movie 2. Real-time images of the PSM of an E10.5 Hes1-Ub1-Luc embryo. Images were taken by 20 min exposure and binning of pixels 4 x 4 over a period of 15 hours. Oscillation was propagated from the caudal end to S0 in the PSM.

Movie 3. Real-time images of dissociated PSM cells from an E10.5 Hes1-Ub1-Luc embryo (top, cell #1; middle, cell #2; bottom, cell #3 in Fig. 4). Images were taken by 10 min exposure and binning of pixels 8 x 8 over a period of 12 hours.